XVIII IMEKO WORLD CONGRESS
Metrology for a Sustainable Development
September, 17 – 22, 2006, Rio de Janeiro, Brazil

DESIGN AND CHARACTERIZATION OF A SUN SENSOR FOR THE SSETI-ESEO PROJECT

Pedro M. Rodrigues [1], *Pedro M. Ramos* [2]

[1] Instituto Superior Técnico, DEEC, Lisboa, Portugal, pedro.mouta@clix.pt
[2] Instituto de Telecomunicações, Instituto Superior Técnico, DEEC, Lisboa, Portugal, pedro.ramos@lx.it.pt

Abstract: Sun sensors are used to measure the orientation of the satellite in orbit using the sun as a reference. This paper includes the preliminary design of a sun sensor, the design and implementation of an automatic testing system and a preliminary characterization of the most important components.

Keywords: SSETI, sun sensor, photodiode, PSD, position sensing detector.

1. INTRODUCTION

The Student Space Exploration and Technology Initiative (SSETI) started from the European Space Agency (ESA) in 2000. SSETI's major goal is to give students from European universities the opportunity to design, build and launch micro-satellites. The project following SSETI Express [1] is the European Student Earth Orbiter (ESEO), an earth observation micro-satellite whose mission is to photograph some European cities, perform radiation measurements and test a thrust vectoring propulsion system.

One of the ESEO subsystems is the Attitude and Orbit Control Subsystem (AOCS) which is responsible for the satellite stabilization, for maintaining a correct orientation during the nominal mission and performing accurate manoeuvres. One of the attitude determination sensors [2] is the sun sensor, the most used in satellite missions in the inner solar system, since it uses a distant and reliable power source as reference, which greatly simplifies the design of these sensors and improves their reliability. A sun sensor uses the sunbeams direction to determine the satellite's orientation.

In this paper, a simple description of the sun sensor's principle of operation is presented as well as the dimensioning and selection of all its components. The main focus will be in the characterization of the photodiode. The testing system used will be presented and the results discussed. The characterization includes testing precision and linearity and determining efficient methods to improve its precision.

2. STATE OF THE ART

Satellite attitude determination is usually made using one large body in space as a reference. The sun and the earth are the most used. Sun sensors, which are usually made using optical devices such as position sensing detectors, use the sun properties, as the light power and the distance, to simplify their operation. Sun sensors can be analog or digital depending on the way the measurements are made. Analog sun sensors use photodiodes to generate one or more analog currents, while digital sun sensors commonly use CCD technology to determine the sun location. With the new Micro Electro Mechanical Systems (MEMS) technology a new generation of sun sensors is also arising [3].

Earth horizon sensors are also optical devices, which use edge detection algorithms to determine the earth horizon position, and are made using photodiode arrays or CCD cameras. Magnetometers are also frequently used in low earth orbit (LEO) missions and measure the direction of the earth magnetic field to compare with the satellite attitude. Recently the use of global positioning system (GPS) is also being studied for LEO satellites [4] which can give extremely high accuracy in attitude determination [5]. Star trackers identify the position of known stars in its field of view and compare them with star catalogues loaded in memory. It also uses CCD to take a picture of the stars and by comparison can detect the displacement of the stars in the picture using star recognition algorithms [6].

Even though the presented sun sensor is an analog sensor in terms of measurement, its output is digital. This sensor is a built-in solution, comprising attitude measurement, analog and digital signal processing and digital communication using Controller Area Network (CAN) protocol.

3. PRINCIPLE OF OPERATION

A sun sensor must primarily convert sunlight energy into an electrical measurement. This is done using a Position Sensing Detector (PSD), which is a photodiode [7] that converts incident light energy into electrical current. In this case a two-dimensional PSD will be used, since the purpose is to measure three-dimensional angles. The PSD performs a sort of integration in the active area and determines the center of the light spot. A pinhole is used to limit the incident light to a smaller beam to increase precision. Figure 1 shows the photodiode principle of operation.

The angular coordinates can be given in terms of elevation (θ) and azimuth (ϕ) which are the attitude angles to be determined by the sensor [8]. As the incident light hits the surface of the photodiode, four electrical currents are generated, proportional to the incident spot position. From these currents it is possible to determine the position of

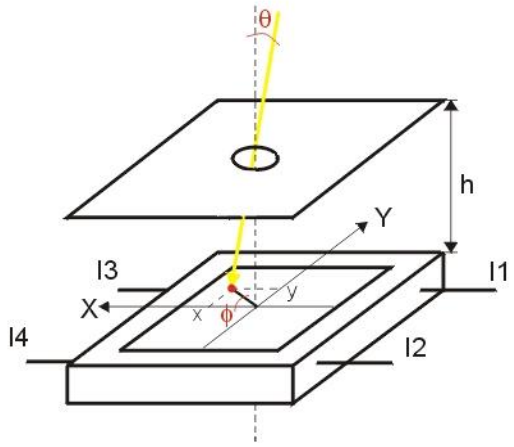

Figure 1 – Transducer principle of operation.

incidence (x,y) using formulas provided by the transducer manufacturer. Having x and y, the coordinates of the incident beam, θ and ϕ can be written as

$$\phi = \arctan\frac{y}{x} \tag{1}$$

$$\theta = \arctan\frac{\sqrt{x^2 + y^2}}{h}. \tag{2}$$

Equation (1) has, however, a singularity, when $x = 0$. This happens for $\phi = \pm\pi/2$, where the sign is given by the sign of y. Equation (2) does not have this problem since the height of the pinhole, h, is fixed and never zero. If both x and y are zero, (1) has no solution. This happens when $\theta = 0$. In this situation, ϕ is not defined. This problem can be solved by first calculating (2) and only calculate (1) if $\theta \neq 0$.

At this point, the attitude angles are in an implicit form, in these four electrical currents. The first electronic stage after the transducer is a transresistance circuit which converts the currents to voltages and amplifies them. The dimensioning of this first stage implies an accurate knowledge about the generated currents' magnitude in order to set the voltages between the desired conversion range. However, it is extremely difficult to predict the magnitude since it depends on the sun spectrum, the PSD spectral response and the beam dimension. The second stage is a programmable gain block which introduces a variable gain to the voltages to adjust them to the A/D range. Finally, a microcontroller is necessary to control the programmable gain block, perform calculations and manage the communication between the sensor and the rest of the satellite. The sun sensor block diagram is shown in Figure 2.

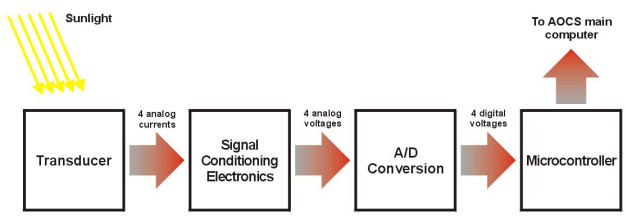

Figure 2 – Sun sensor simplified block diagram.

4. DESIGN

The chosen photodiode is the Hamamatsu S5991-01. It has an active area of (9×9) mm, a position resolution of 1.5 µm and an operating temperature range from - 20ºC up to + 60ºC, which is relevant in space applications. The pinhole has a diameter of 400µm, large enough to avoid significant diffraction perturbations but not too large to avoid heat generation near the photodiode and allow a good resolution.

The sun sensor's field of view (FOV) geometry is a rectangular pyramid with a 120º angle between opposite sides and 135º in the diagonals (Figure 3). The width of the FOV is determined by the distance between the pinhole and the photodiode. As the FOV increases, the necessary resolution in the photodiode also increases, which could be a problem if the photodiode position resolution is exceeded. For this photodiode and FOV this is not a problem, however one possible solution could be using multiple pinholes with smaller fields of view [9]. The number and placement of the sun sensors in the satellite will ultimately determine their overall coverage [10].

The generated current depends on the sun spectrum, the photodiode spectral response and the pinhole diameter. The current is given by

$$I = A_{pin}\int_{\lambda} I_r(\lambda)R(\lambda)d\lambda\,, \tag{3}$$

where A_{pin} is the pinhole area, I_r is the sun spectral irradiance and R is the photodiode spectral response. Since the last two are fixed, the generated current is directly dependent on the pinhole diameter. The chosen diameter is 400 µm which is enough to avoid considerable diffraction effects [11] and to generate a small beam, increasing accuracy. The estimated total generated current is approximately 50 µA.

The currents generated by the photodiode pass through a transresistance amplifier with a low-pass filter (Figure 4). This first gain stage is designed to convert the small generated currents to voltages close to the A/D converter range. The transimpedance gain is fixed to 20000 Ω and the low-pass filter cut-off frequency to 10 Hz, which should be enough to filter high frequency noise while maintaining an acceptable time constant. The outputs of these stages are four voltages with a maximum magnitude of 1 V.

However, since the currents depend on the incidence position, their magnitude will not be equal. Moreover, in some cases, some of the voltages will still have very low magnitudes. To achieve maximum resolution in A/D conversion, all voltages shall be close to the A/D converter range. To improve resolution and also to compensate

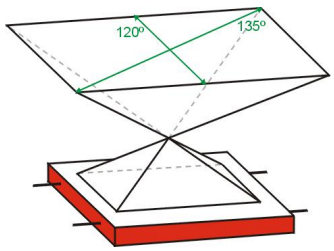

Figure 3 – Sun sensor's field of view geometry.

for the sun power variation along the orbit, a variable gain stage is introduced, using digital potentiometers. The stage gain is digitally controlled and the output is given by

$$V_0 = \left(1 + \frac{n}{255 - n}\right) V_I , \tag{4}$$

where n is a digital parameter regulated by the microcontroller.

The chosen A/D converter is the MAX147 from Maxim with a 12-bit resolution and 4 differential input channels, which is convenient, for the four voltages. It has low power consumption, which is also important to keep within the mission power budget. The input voltage range is between 0 and 2.5 V. These converters use a successive-approximation conversion (SAR) technique.

After A/D conversion, a microcontroller calculates the incidence position (x,y) using two equations provided by the photodiode manufacturer:

$$\frac{2x}{L} = \frac{(I_2 + I_3) - (I_1 + I_4)}{I_1 + I_2 + I_3 + I_4} \tag{5}$$

$$\frac{2y}{L} = \frac{(I_2 + I_4) - (I_1 + I_3)}{I_1 + I_2 + I_3 + I_4} , \tag{6}$$

where $L = 9$ mm. These values are then sent to the AOCS main computer, using CAN protocol, where the attitude angles are determined and used in the control algorithms. This microcontroller also operates the digital potentiometers and the A/D conversion. Based mainly on the communication requirements, the chosen microcontroller is the Dallas Maxim DS80C390. It has two CAN 2.0B controllers which is compatible with the nominal and redundant lines for the data interface with the satellite.

The full sun sensor electronic circuit is shown in Figure 4.

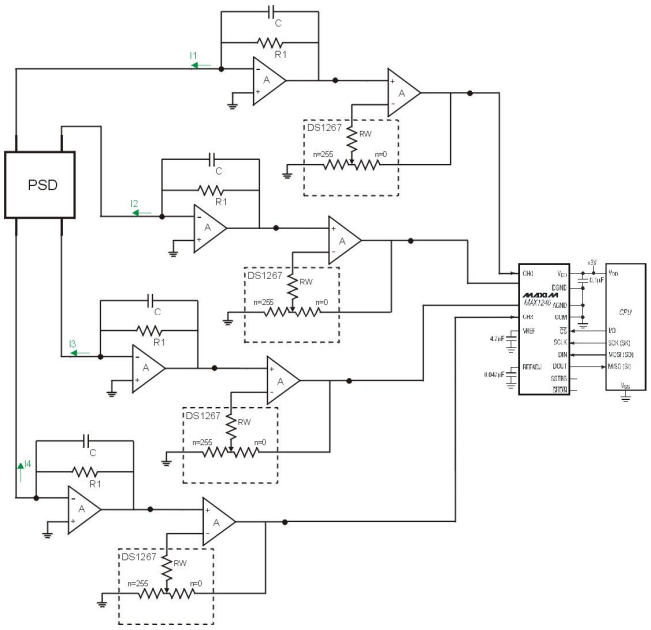

Figure 4 – Sun sensor electronic circuit.

5. TESTING SYSTEM

To simulate the operating conditions of the sun sensor it is important, first of all, to simulate the Sun, as close as possible, and to find a way to simulate all the possible light incidence angles. The transducer must be isolated from any other light sources and it should be possible to change its field of view. Finally, the data generated by the section of the sun sensor which is to be characterized must be acquired.

The first challenge is to simulate the sun itself. It can be simulated in terms of irradiance, radiation spectrum or beam geometry. If it was possible to have a light source with the same spectrum as the Sun it would be possible to determine experimentally the current previously dimensioned. However, it is extremely difficult to find a light source with such a complex spectrum. The decision was not to simulate the exact spectrum but to produce an average sun irradiance disregarding the wavelengths involved. Of course, this will not give an accurate measure due to the transducer's spectral response, but it is possible to achieve a good estimate. The most suitable light source to simulate the Sun, commercially available, is an halogen lamp with a reflecting parabola. Halogen lamps usually have high irradiance and the reflecting parabola helps to reduce the divergence of the emitted light. The chosen lamp is the 150 W Philips 13117. No data was available concerning beam divergence. The sun, at this distance, has a divergence of approximately 0.1º. Experimental tests made to the halogen lamp showed a divergence of 5.5º which is reasonable for this preliminary characterization and very good for a commercial lamp.

The testing system must be able to change its direction of incidence with an angular precision better or equal to the desired sun sensor measurement precision, i.e. 0.1º. The idea is to have a stepper motor with a step angle equal to the wanted precision, which gives the automatic measuring ability on one dimension. The other degree of freedom is given by a manual variation of the transducer orientation.

The chosen stepper motor is the Jameco 30BYJ02AH. It is an unipolar stepper motor with a step angle of 0.09º, works with 12 VDC and has a maximum winding current of 60 mA. The motor control is done by creating a torque in the rotor by alternately energizing each of the motor windings' halves. The stepper motor control implemented (Figure 5) consists of four MOS transistors working as analog switches, allowing or not the current to flow across the windings. The diodes protect the transistors from voltage spikes during transitions. Depending on the digital sequence applied the motor can operate in full step or half step mode (0.09º).

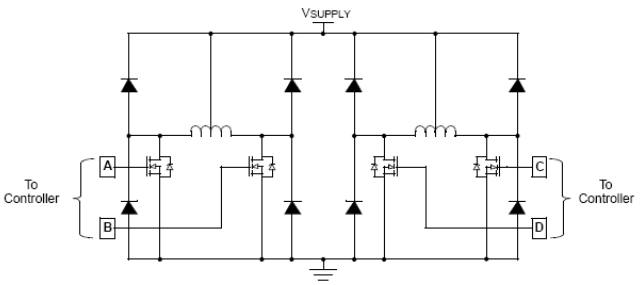

Figure 5 – Stepper motor control circuit.

The halogen lamp is adapted to the stepper motor shaft using an aluminium piece which allowed changing the distance to the light source. With this system it is possible to perform an automatic measurement along one axis of the photodiode, changing the incidence angle in steps of 0.09º.

An aluminium box was built to limit the light in the transducer. It has the pinhole on the top face, parallel to the photodiode surface. It also has the possibility to change the height between the pinhole and the transducer, thus allowing to choose the field of view. This box has another feature which gives the testing system the second degree of freedom to simulate light incidence direction. It allows the whole system (pinhole+transducer) to rotate around an axis perpendicular to and centered with both. However, this must be done manually. The idea is to perform automatic measurements along one direction, rotate the box by a known angle and run the automatic measurement again.

The portion of the sun sensor under test is the photodiode and the first transimpedance gain stage, mounted in breadboard. The full testing system setup is shown in Figure 6.

To acquire data generated by the photodiode, a data acquisition unit is used and the global control of the system is done using a computer and LabVIEW software. To acquire the four voltages a USB data acquisition unit from National Instruments (NI-DAQmx USB-6008) was used. It has four differential input channels and 12 bit resolution for the analog measurements and eight digital outputs for the motor control. The maximum sample rate is of 2.5 kHz for each channel.

6. CHARACTERIZATION

The characterization is focused on determining the PSD behaviour. However, since the currents generated are so small and thus hard to measure, there is the need to include the first gain stage into the characterization as well. The main objective is to see if the sensor is linear in the position, i.e. if the relation between the incidence angle (or its tangent to be more precise) and the position measured by the photodiode is linear, which would also allow to determine any systematic errors, like offsets in the transducer or misalignments in the testing system.

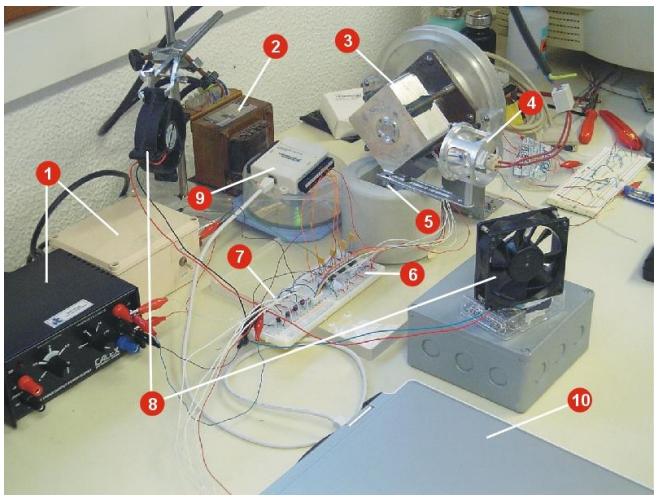

Figure 6 – Testing system setup: 1 – Power sources; 2 – Halogen lamp transformer; 3 – Transducer box; 4 – Halogen lamp; 5 – Stepper motor; 6 – Signal conditioning electronics; 7 – Stepper control circuit; 8 – Cooling fans; 9 – Data acquisition unit; 10 – Laptop computer.

The first results obtained are represented in Figure 7 and show the incidence positions of the light in the PSD surface. The lines represent different tests for different azimuth angles, ϕ (0º, 45º, 90º, -45º). Each line represents a variation of the elevation angle, θ, from -60º to 60º.

There is an offset in position due to the photodiode offset and the test setup. The geometrical center is different from the electrical center. This can be seen in Figure 6 where the lines are not centered with the PSD surface.

The main goal of the characterization is to determine the relation between the incident angles and the position measured by the sensor. As mentioned in the previous section, ϕ is fixed for each automatic variation of θ and only four different measures where made, which means that this characterization is focused on the elevation angle. Rewriting (2) it is possible to find the linear relation between the tangent of the incidence angle and the measured position. It is given by

$$\tan\theta = \frac{1}{h}\sqrt{x^2 + y^2} \ . \qquad (7)$$

However, this geometric model is only valid when the pinhole and the transducer are perfectly centered. To take into account the offsets, the adjusted model is

$$\tan\theta = \frac{1}{h}\sqrt{(x - x_0)^2 + (y - y_0)^2} \ , \qquad (8)$$

where x_0 and y_0 are the offsets in both directions. This relation suggests a linear relation between the tangent of the elevation angle and the corrected coordinates given by the transducer along the principal axis.

Figure 8 shows the results obtained for an azimuth angle of -45º. First, a small note about the data manipulation done to obtain this figure: by definition, θ is always a positive angle (Figure 1). However, to give a better perspective of the photodiode behaviour, it was necessary to simulate a transition to an hypothetical negative value of θ. That is the reason for having the *sign(θ)* in Figure 8.

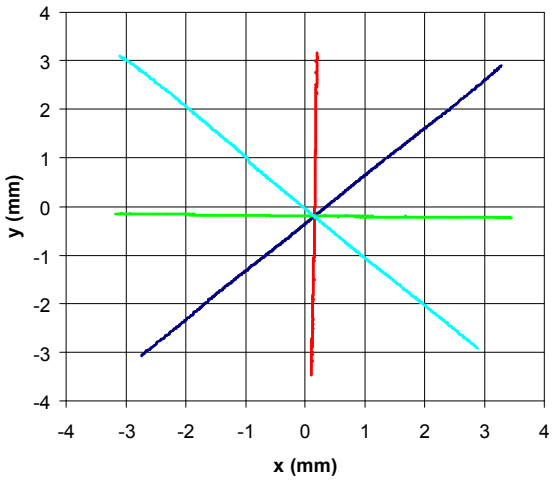

Figure 7 – Incidence position of the light during tests.

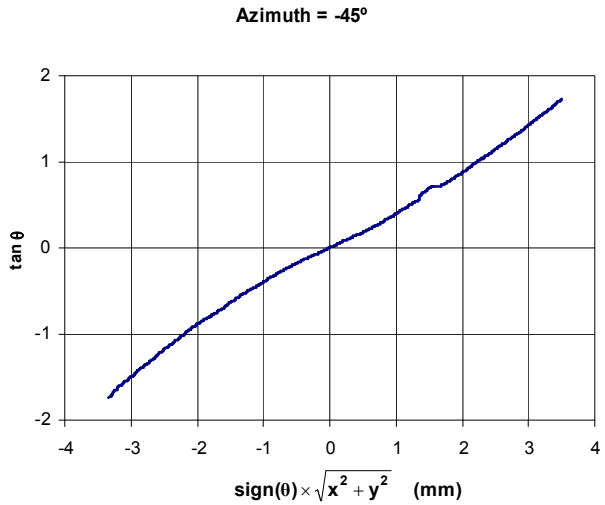

Figure 8 – Relation between incident position and incidence angle.

It is possible to see that the transducer has a linear behaviour only close to the center, while near the edges it starts to curve. There is also a small portion of the results that is not coherent with the rest. This small deviation is present in every measurement made, in the same place, which suggests a defect in the photodiode active area. This portion is not considered hereafter.

The next step is to find a polynomial which best interpolates the curve in Figure 8. The criterion used is the minimization of the maximum error between the true angle and the measured angle, obtained in the test, i.e. the polynomial which has the minimum

$$\max\left(\hat{\theta}-\theta\right)^2. \qquad (9)$$

The determination of the best polynomial coefficients was made using a nonlinear minimization algorithm implemented in MATLAB. The algorithm starts from an initial estimate given by the user and runs a search algorithm to find a minimum of the given cost function (9) given some stop criteria. However, the algorithm can only find a local minimum of the function, which is a limitation. Taking this into account, it is important to give a good initial estimate, since this will define the search area of the solution space.

The first approach was to consider always a linear initial estimate regardless the polynomial order, which gives unexpected results. The maximum error does not decrease with the polynomial order, meaning the algorithm is searching in different regions, each time it is executed for a different polynomial order. The second approach was to keep the last polynomial order coefficients estimated by the algorithm and use them as the initial estimate when running the algorithm for the next order.

Figure 9 shows the evolution of the maximum angle error given by (9) as a function of the polynomial order for the second approach. It is possible to see that, when using the last estimate, the results are significantly better, since the algorithm will look always in the same region, gradually adding degrees of freedom to better interpolate the curve given (Figure 8).

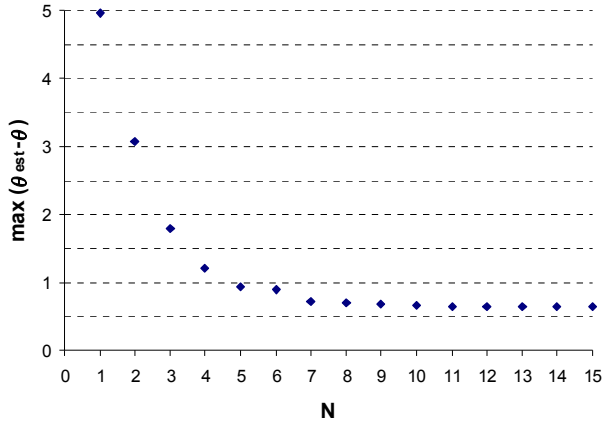

Figure 9 – Relation between maximum error and polynomial order, using the last order coefficients as initial estimate.

With this method the maximum error is reduced almost ten times at order 15, comparing with the linear approach, obtaining an error smaller than 0.65º. It is important to recall, however, that this may not be the best solution for the given data, since the algorithm can only assure a local minimum.

7. CONCLUSIONS

In this paper, the principle of operation of a sun sensor was described and the design considerations were presented. A low-cost testing system for the preliminary photodiode characterization was presented and characterization results and error minimization techniques were introduced.

Since this is an ongoing project, further work will be made in this area, especially as the resolution needed for the sun sensor (0.1º) was not yet achieved. Next step will be the implementation of the circuit in a PCB to reduce noise and the exploration of other minimization algorithms to reduce the sensor error. The analysis of the uncertainty components of the sensor as a function of the sun position is still being made. The development of a more accurate and reliable testing system is also being considered.

REFERENCES

[1] L. Alminde et al, "The SSETI-express mission: from idea to launch in one and a half year", Proc. of 2nd International Conference on Recent Advances in Space Technologies, pp. 100-105, June 2005.

[2] M. E. Koniger, "Sensors for space applications", Proc. of VLSI and Computer Peripherals. VLSI and Microelectronic Applications in Intelligent Peripherals and their Interconnection Networks, pp 3/68-3/73, 8-12 May 1989.

[3] Dr. C. C. Liebe, Dr. S. Mobasser, "MEMS based sun sensor", Aerospace Conference, IEEE Proceedings Vol.3, pp 3/1565-3/1572, March 2001.

[4] X. Yu, K. Ling, N. Nagaragan, "LEO Satellite Attitude Determination based on GPS", Proceedings of the 38th IEEE Conference on Decision and Control Vol.2, pp. 1988-1992, December 1999.

[5] E.F. Stefatos, T. Arslan, “High-Performance Adaptive GPS Attitude Determination VLSI Architecture”, IEEE Workshop on Signal Processing System (SIPS) 2004, pp. 233-238, 2004.

[6] G. L. Rosseau, J. Bostel, B. Mazari, “Star recognition algorithm for APS start tracker”, IEEE Aerospace and Electronic Systems Magazine Vol.20, Issue 2, pp. 27-31, February 2005.

[7] S. Chamberlain, “Photosensitivity and Scanning of Silicon Image Detector Arrays”, IEEE Journal of Solid State Circuits, vol. sc-04, n. 6, December 1969.

[8] R. Doraiswami, S. Price, “A robust position estimation scheme using sun sensor”, IEEE Transactions on Instrumentation and Measurement, vol. 47, Issue 2, pp. 595-603, April 1998.

[9] C. C. H. Ma, C. K. Tan, P. D. Lawrence, “Multi-Pinhole Wide-Angle High-Resolution Light Position Detector”, IEEE Transactions on Instrumentation and Measurement Vol. 45, Issue 1, pp 195-200, February 1996.

[10] B. Jackson, B. Carpenter, “Optimal Placement of Spacecraft Sun Sensors Using Stochastic Optimization”, Proc. of IEEE Aerospace Conference, pp. 3916-3923, 2004.

[11] K. D. Mielenz, “Algorithms for Fresnel Diffraction at Rectangular and Circular Apertures”, Journal of Research of the National Institute of Standards and Technology Vol. 103, Nº 5, September-October 1998.